Jagannath University Journal of Science
Volume 08, Number I, December 2021, pp. 33–44
https://jnu.ac.bd/journal/portal/archives/science.jsp
ISSN 2224-1698

JnUJSci

Unsteady Features of Laminar Viscous Incompressible Flow and Temperature Dissemination through a Rotating Bent Rectangular Channel: The Case of Negative Rotation

Research Article

Sreedam Chandra Adhikari[1], Mohammad Sanjeed Hasan[2], Rabeya Akter[1], Rabindra Nath Mondal[1]*

[1]*Department of Mathematics, Jagannath University, Dhaka-1100, Bangladesh*
[2]*Department of Mathematics, Bangabandhu Sheikh Mujibur Rahman Science and Technology University, Gopalganj, Bangladesh*

Received: 02 February 2021
Accepted: 14 October 2021

Abstract: The current study investigates the effects of rotation on fluid flow and heat transfer through a curved channel of rectangular cross-section with bottom wall heated and cooling from the top. A wide range of the Taylor number, $-500 \le Tr \le 0$ with constant curvature δ = 0.2, aspect ratio 2 and the Prandtl number Pr = 7.0 (water) have been considered for the study. After a broad investigation to explore transient flow behavior, time-history analysis is performed using phase trajectory of the transient solutions at fully developed stage. As a result, the stages of transient flow endure in the consequence "*chaotic* → *periodic* → *multi-periodic* → *chaotic*" for the rotating system in the negative direction comprising with 2- to 8-vortex solutions. It is further illustrated from stream function and energy distribution that the heat transfer is ominously enhanced at high rotation and the chaotic flow enhances heat transfer more significantly than the steady-state, periodic or other physically realizable solutions. Finally, the current numerical results are compared with laboratory-based experimental results and a good agreement is observed.

Keywords: *Rotating bent duct • Flow pattern • Unsteady solution • Phase-plot • Heat transfer.*

1. Introduction

The topic of investigation in fully developed fluid flows and heat transfer through rotating bent channel like constrained domains is of essential interest of plentiful investigators since the multiplicity of numerous applications in the engineering fields exempli gratia in transporting fluids, rotating-machinery, nuclear engineering, heat exchangers, gas turbines, electric generators etc.. It is noted that there have been a number of studies and review articles on hydrodynamic unpredictability and heat transfer on rotating curved duct with various geometries from last two or three decades. At an exact flow condition, Dean vortices appearing near the outside bowl-shaped wall of the channel, called by the name of Dean (1927). After that, significant studies on analytical, numerical and experimental inquiries have been done; here the researches are mentioned to Mondal *et al*. (2006, 2007a), Yamamoto *et al*. (2006), Zhao *et al*. (2020) and Nowruzi *et al*. (2019) for a number of excellent reviews on curved channel flows.

It is worth mentioning that generally there exist many steady and unsteady flow characteristics which are imposed by the curvature and rotation of the duct. A mathematical exploration of fluid flow through a rotating

*Corresponding author: Rabindra Nath Mondal
Email: rnmondal71@yahoo.com

curved pipe of spherical and rectangular cross-section was accomplished by Miyazaki (1971, 1973). Ludwieg (1951) implemented integral based technique in the rotating curved duct to study the flow characteristics. Wang and Chang (1996) used finite volume method to observe the secondary flows of the curved rectangular duct for co-rotating cases. Zhang *et al*. (2001) investigated the centrifugal force and aspect ratio effects in the presence of the friction factor through the curved duct. Wang and Yang (2004) demonstrated the displacements of the bifurcation for increasing the truncation numbers. Hasan *et al*. (2019) adopted the spectral method to analyze the critical points for both rotating and non-rotating curved ducts. However, despite the above-cited papers on discussion for critical, limit points of bifurcation, the papers did not illustrate the structural change of secondary vortices in limit and critical points. The ongoing study minimizes these gaps.

It is significant to discuss about the unsteady flow characteristics through curved channels which can be implemented in many industrial equipment including pump machine, computer chip, water reactor. Yanase and Nishiyama (1988) performed oscillating behavior of curved duct flows for rectangular cross-section. Related to oscillating behavior in a confined geometry, e.g. rectangular duct or channel, several works have been conducted. Recently Mondal *et al*. (2017) and Yanase *et al.* (2008) investigated the regular and irregular oscillation with identifying the symmetry and without symmetry condition in flow behaviors respectively. Wang and Yang (2004, 2005) reported an extensive study with numerical analysis for determining oscillation behaviors of the flow through the square shaped curved duct. They further performed this work experimentally by considering flow visualization technique. Yamamoto *et al.* (2006) performed Taylor-Dean flow visualization method to study secondary flow characteristics in a curved rotating duct experimentally. Mondal *et al*. (2010, 2015a) analyzed numerical prognosis of the oscillation behavior by time advancement for flow considering square and rectangular configurations and discussed detailed transitions between periodic and aperiodic oscillating and instability of the oscillating behavior (Mondal *et al*, 2016). Nowruzi *et al*. (2019) applied Homotopy perturbation method to investigate hydrodynamic instability in a curved channel of different aspect ratio for several curvatures. Recently, Zhao *et al*. (2020) illustrated the influence of friction factor and Nusselt number in terms of time instead of large Reynolds numbers and curvature ratios. Mondal *et al*. (2013, 2014) and Hasan *et al*. (2019, 2020) demonstrated the structural change of flow velocity and isotherms in terms of changing the time. However, their study was unable to focus the influence of the parameters in flow transition and velocity profile. Very recently, Mondal *et al.* (2021) conducted numerical prognosis of the oscillating behavior by time-advancement for considering the rectangular configurations and discussed detailed transitions between periodic and aperiodic oscillating and instability of the oscillating behavior in a rotating system. Among the above cited articles, however, the effects of rotation in fluid flow as well as unsteady behavior is still absent in literature for a rotating curved rectangular duct flow of moderate aspect ratio; which motivated the current study to refill this gap.

To study heat transmission in the curved channel, numerical schemes to describe the spiraling fluid flow properties and heat transfer through the rectangular and elliptical duct have been conducted by Chandratilleke and Nursubyakto (2003). Very recently, Zhang *et al*. (2020) represented the heat transfer effects in a channel flow for changing the Reynolds and rotational number and the temperature ratios. Nobari *et al.* (2009) calculated the heat transfer for both curved and straight annular duct and finally, they found a fixed range of thermal conductivity point where the heat transfer for both curved and annular duct was equal. Bibin and Jayakumar (2020) enumerated the hydrodynamic flow characteristics in the presence of heat generation through a duct where a porous material was put at the duct center. Zhao *et al.* (2020) formed a correlation between the Nusselt number and friction factor by regression analysis through helical duct for an extensive range of Reynolds number and curvature ratios. Abu-Hamdeh *et al.* (2020) considered the flow regimes as turbulent and showed that the heat exchangers are more effective in the semicircular tube than the quadrant-circular and tube-in-tube cross-section. Hasan *et al.* (2019, 2020) recently conducted finite element analysis to illustrate the total heat transfer through square duct for a large number of the Dean and Taylor numbers. They obtained different types of critical flow behaviors in both steady and unsteady solutions within the range of the required parameters. Very recently, Adhikari *et al*. (2021) performed spectral-based numerical study to characterize pressure-induced instability characteristics of a transient flow and energy distribution through a bent square duct with small curvature. Chanda *et al*. (2021a, 2021b, 2021c) adopted spectral method to investigate flow behavior and energy distribution through a rotating curved rectangular channel with various curvatures. However, a complete behavior of transient solution with the results of heat-flux effect on flow evolution is still absent in literature; which attracted the authors to fill up this gap.

In this study, the development of the complex flow behaviors in the thermal flow transition in a rectangular channel with stream-wise curvature while identifying the

influence from the various flow and geometrical parameters are investigated for different Taylor numbers in the negative direction. The main purpose of this study is to explore transient behavior with heat-flux properties of secondary vortices on the heat transfer. The study articulates and verifies an advanced approach for computational scheme to identify hydrodynamic variability in a curved rotating duct reflected by the generation of Dean vortices.

2. Governing Equations and Flow Model

Consideration is given for fully developed two-dimensional (2D) flow which passes through a curved square duct (CSD). Figure 1 illustrates the cross-sectional view and the coordinate system of the computational domain with necessary notations. The bottom and top edges of the working system are considered to be heated and cooled respectively; the upright walls are well insulated to prevent any heat loss. The fluid passes through consistently in the stream-wise direction as shown in Figure 1.

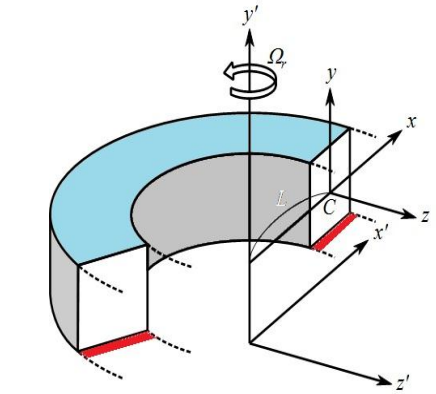

(a)

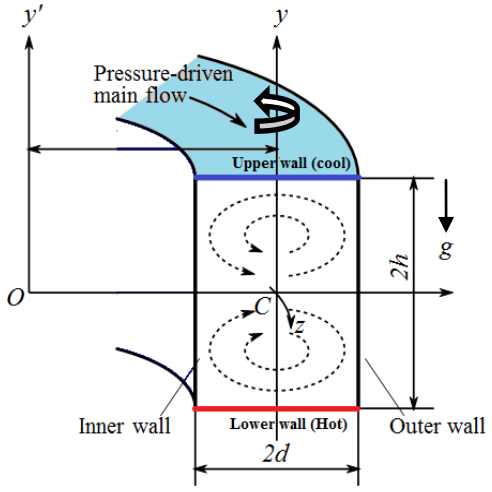

(b)

Figure 1. (a) Coordinate system, (b) Cross-sectional view

The stream functions for cross-sectional velocities have the following form

$$u=\frac{1}{r}\frac{\partial\psi}{\partial y},\quad v=-\frac{1}{r}\frac{\partial\psi}{\partial x}\Bigg\} \tag{1}$$

where, $r=1+\delta x$.

Now, axial velocity (w), stream function (ψ) and isotherms (T) are derived with non-dimensional parameters in the Navier-Stokes and energy equations which are expressed as

$$(1+\delta x)\frac{\partial w}{\partial t}=Dn-\frac{1}{2}\frac{\partial(w,\psi)}{\partial(x,y)}-\frac{\delta^2 w}{1+\delta x}$$

$$-\frac{\delta^2 w}{1+\delta x}+(1+\delta x)\Delta_2 w-\frac{\delta}{2(1+\delta x)}\frac{\partial\psi}{\partial y}w+\delta\frac{\partial w}{\partial x}-\delta Tr\frac{\partial\psi}{\partial y} \tag{2}$$

$$\left(\Delta_2-\frac{\delta}{1+\delta x}\frac{\partial}{\partial x}\right)\frac{\partial\psi}{\partial t}=-\frac{1}{2(1+\delta x)}\frac{\partial(\Delta_2\psi,\psi)}{\partial(x,y)}$$

$$+\frac{\delta}{2(1+\delta x)^2}\left[\frac{\partial\psi}{\partial y}\left(2\Delta_2\psi-\frac{3\delta}{1+\delta x}\frac{\partial\psi}{\partial x}+\frac{\partial^2\psi}{\partial x^2}\right)\right.$$

$$\left.-\frac{\partial\psi}{\partial x}\frac{\partial^2\psi}{\partial x\partial y}\right]+\frac{\delta}{(1+\delta x)^2}\left[3\delta\frac{\partial^2\psi}{\partial x^2}-\frac{3\delta^2}{1+\delta x}\frac{\partial\psi}{\partial x}\right]$$

$$-\frac{2\delta}{1+\delta x}\frac{\partial}{\partial x}\Delta_2\psi+\frac{1}{2}w\frac{\partial w}{\partial y}+\Delta_2{}^2\psi$$

$$-Gr\ (1+\delta x)\frac{\partial T}{\partial x}+\frac{1}{2}Tr\frac{\partial w}{\partial y}, \tag{3}$$

$$\frac{\partial T}{\partial t}=\frac{1}{\mathrm{Pr}}\left(\Delta_2 T+\frac{\delta}{1+\delta x}\frac{\partial T}{\partial x}\right)-\frac{1}{2(1+\delta x)}\frac{\partial(T,\psi)}{\partial(x,y)} \tag{4}$$

The dimensionless parameters, the Dean number Dn; the Grashof number Gr; the Prandtl number Pr and the Taylor number Tr are addressed as:

$$Dn=\frac{Gd^3}{\mu\upsilon}\sqrt{\frac{2d}{L}},\ Gr=\frac{\beta g\Delta T d^3}{\upsilon^2},\ Tr=\frac{2\sqrt{2\delta}\Omega_T d^3}{\upsilon\delta},\ \mathrm{Pr}=\frac{\upsilon}{\kappa} \tag{5}$$

The boundary conditions for w, ψ and T are applied as:

$$\left.\begin{aligned} w(\pm1,y)=w(x,\pm1)=\psi(\pm1,y)=\psi(x,\pm1)=0,\\ \frac{\partial\psi}{\partial x}(\pm1,y)=\frac{\partial\psi}{\partial y}(x,\pm1)=0,\\ T(x,1)=1,T(x,-1)=-1,T(\pm1,y)=-y. \end{aligned}\right\} \tag{6}$$

3. Numerical Analysis

3.1 Method of numerical design

For finding the numerical results from equations (2) – (4), spectral technique along with expansion by polynomial functions and Chebyshev polynomials is

applied at the obtained dimensionless momentum and energy equations. That is, the functions expansion of $\phi_n(x)$ and $\psi(x)$ are articulated as:

$$\varphi_n(x)=(1-x^2)C_n(x),\quad \psi_n(x)=(1-x^2)^2C_n(x) \tag{7}$$

where, $C_n(x)=\cos\left(n\cos^{-1}(x)\right)$ is the n^{th} order Chebyshev polynomial, $w(x,y,t)$, $\psi(x,y,t)$ and $T(x,y,t)$ are expanded in terms of $\varphi_n(x)$ and $\psi_n(x)$ as

$$\left.\begin{aligned} w(x,y,t)&=\sum_{m=0}^{M}\sum_{n=0}^{N} w_{mn}(t)\varphi_m(x)\varphi_n(y),\\ \psi(x,y,t)&=\sum_{m=0}^{M}\sum_{n=0}^{N} \psi_{mn}(t)\psi_m(x)\psi_n(y),\\ T(x,y,t)&=\sum_{m=0}^{M}\sum_{n=0}^{N} T_{mn}(t)\varphi_m(x)\varphi_n(y)-y. \end{aligned}\right\} \tag{8}$$

To obtain the steady solutions, the expansion series (8) with coefficients w_{mn}, ψ_{mn} and T_{mn} are substituted into the basic equations (2) - (4) abide by applying the collocation method. To get the unsteady solutions, the Crank-Nicolson and Adams-Bashforth methods together with the function expansion (8) and the collocation methods are applied to equations (2) to (4). The (for details, see Mondal *et al*. 2007a).

3.2 Resistance Coefficient (λ)

The resistant coefficient λ, sometimes noticed as the *hydraulic resistance coefficient*, represented as

$$\frac{P_1^*-P_2^*}{\Delta z^*}=\frac{\lambda}{d_h^*}\frac{1}{2}\rho\left\langle w^*\right\rangle^2 \tag{9}$$

where d_h^* is the hydraulic diameter. The main axial velocity $\left\langle \omega^*\right\rangle$ is defined as

$$\left\langle w^*\right\rangle=\frac{\nu}{4\sqrt{2\delta}d}\int_{-1}^{1}dx\int_{-1}^{1}\bar{w}(x,y,t)\,dy \tag{10}$$

and λ is related to the mean non-dimensional axial velocity $\langle w\rangle=\sqrt{2\delta}d\left\langle w^*\right\rangle/\upsilon$ expressed as

$$\lambda=\frac{16\sqrt{2\delta}Dn}{3\langle w\rangle^2}. \tag{11}$$

3.3 Numerical Accuracy

Grid efficiency study is performed for the parameters (*Dn*, *Gr* and *Tr*) which considered in the present work. For the rectangular duct, we have choose $N = 2M$ for fine mesh grids. We have analyzed several values of truncation numbers *M* and *N* within a range of 14 - 22 for *M* and 28 - 44 for *N*. Five different grid resolutions 14×28, 16×32, 18×36, 20×40 and 22×44 are considered to evaluate the grid sensitivity of the results and to obtain an optimum grid resolution. Table 1 summarizes the parameters for the 5 test cases. A grid with dimensions of 20×40 is used for sufficient accuracy.

Table 1. The values of λ and *w*(0, 0) for various values of the truncation numbers *M* and *N* at *Dn* = 500, *Gr* = 500, *Tr* = -200 and the curvature 0.2

M	*N*	λ	*w* (0, 0)
14	28	0.3431509495	1069.544566
16	32	0.3432371976	1070.025634
18	36	0.3433102861	1070.551156
20	**40**	**0.3433202265**	**1070.720377**
22	44	0.3433191600	1070.749269

4. Results and Discussion

4.1 Unsteady solutions

In the present investigation, the transitional characteristics of the flow in a curved duct which is rotated in the negative direction ($-500 \le Tr \le 0$) and executed under a constant temperature difference, *Gr* = 500, curvature 0.2. Figures 2(a), 4(a), 6(a), 8(a), 10(a), 12(a) and 14(a) respectively show time-dependent results for *Tr* = 0, -50, -100, -200, -335, -340 and -400 successively. As shown in Figures 2(a) and 4(a), the unsteady solutions at *Tr* = 0 and *Tr* = - 50 are chaotic oscillations, Figure 6(a) is a periodic oscillation at *Tr* = -100 and Figures 8(a) and 10(a) are multi-periodic oscillations for *Tr* = - 200 and *Tr* = -335 consecutively. It is also found that Figures 12(a) and 14(a) represent chaotic oscillations again for *Tr* = - 340 and *Tr* = - 400. These chaotic, periodic and multi-periodic oscillations are well justified by sketching phase space trajectories of the time-dependent solutions as shown in Figures 2(b), 4(b), 6(b), 8(b), 10(b), 12(b) and 14(b), respectively. The phase space trajectory analyzes the flow in the $\gamma-\lambda$ plane where $\gamma=\iint\psi\,dxdy$ and this value is null at the center of the duct. The phase space trajectories well justify the nature of flow bevahior.

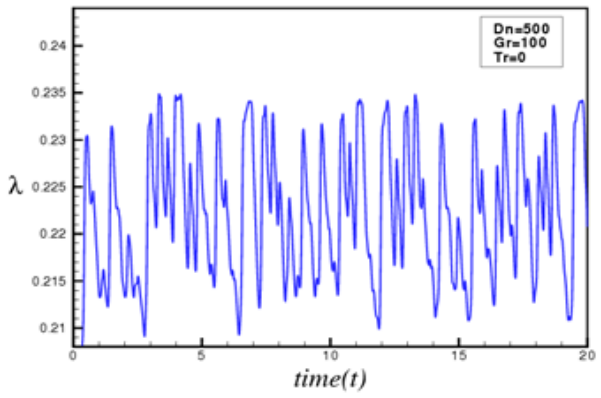

(a)

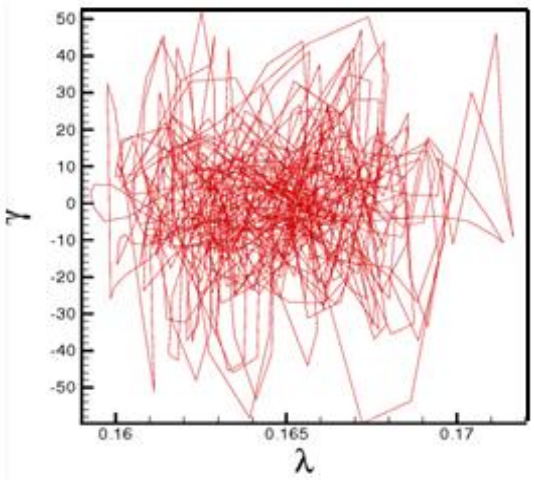

(b)

Figure 2. (a) Chaotic flow characteristics, (b) Phase trajectory for $Tr = 0$.

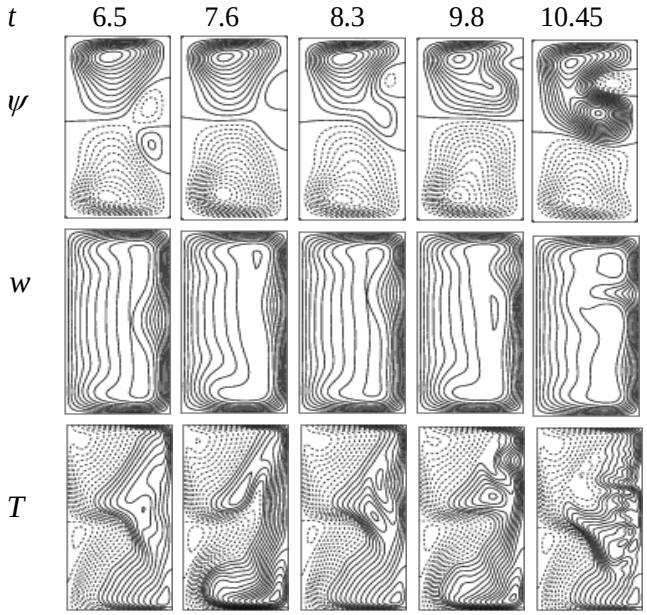

Figure 3. Streamlines of secondary flow (ψ), axial flow (w) and isotherm (T) at different time (t) for $Tr = 0$.

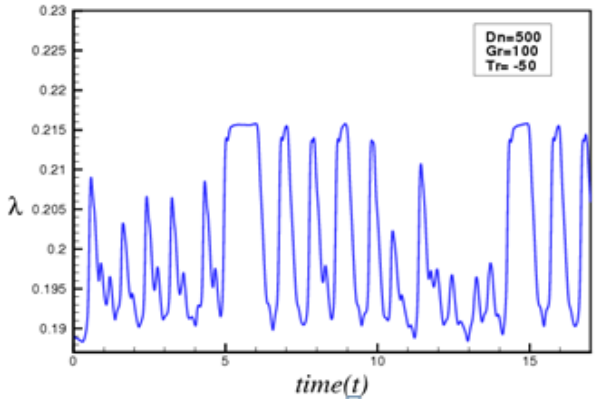

(a)

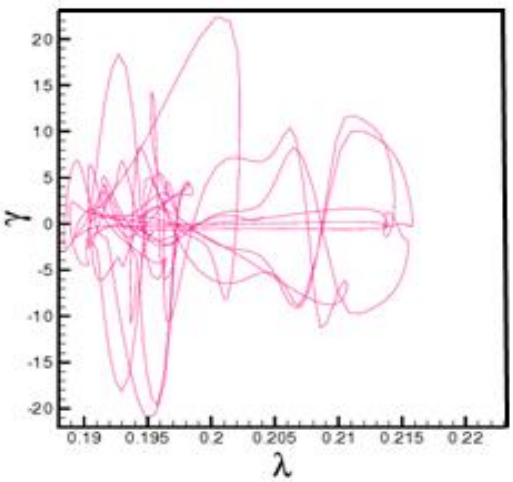

(b)

Figure 4. (a) Chaotic flow characteristics, (b) Phase trajectory for $Tr = -50$.

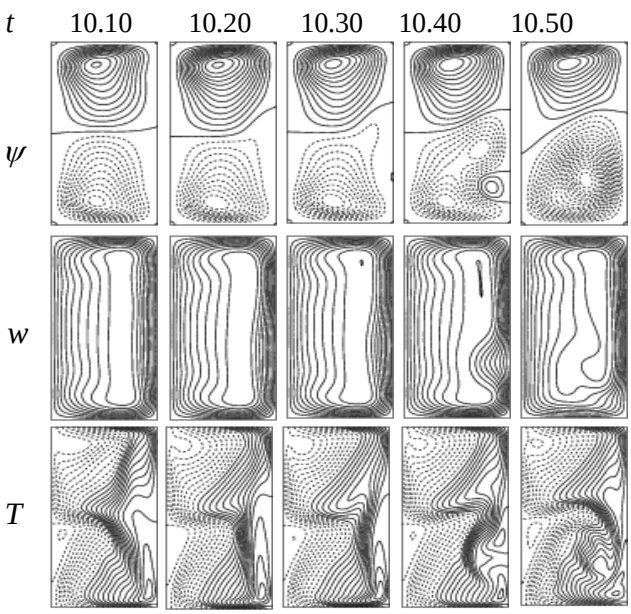

Figure 5. Streamlines of secondary flow (ψ), axial flow (w) and isotherm (T) for different time (t) at $Tr = -50$.

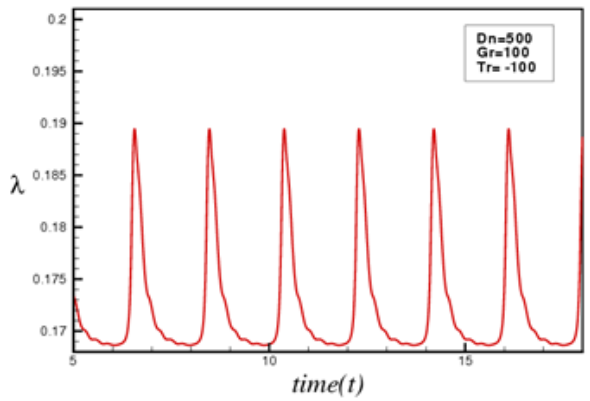

(a)

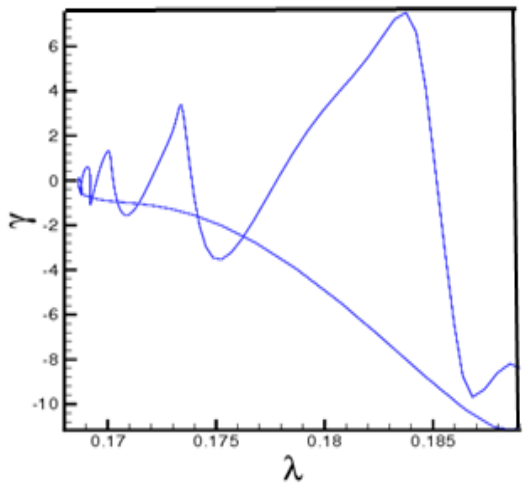

(b)

Figure 6. (a) Periodic flow characteristics (b) Phase trajectory for $Tr = -100$.

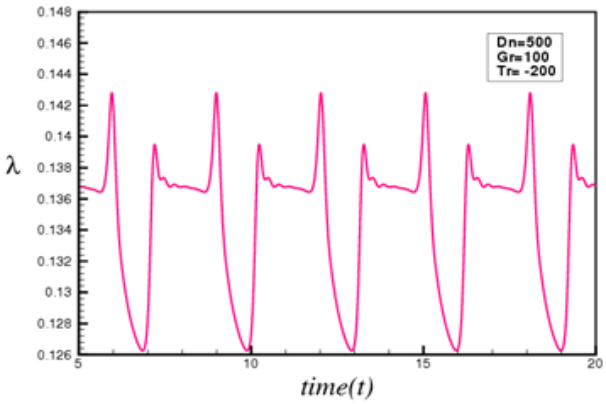

(a)

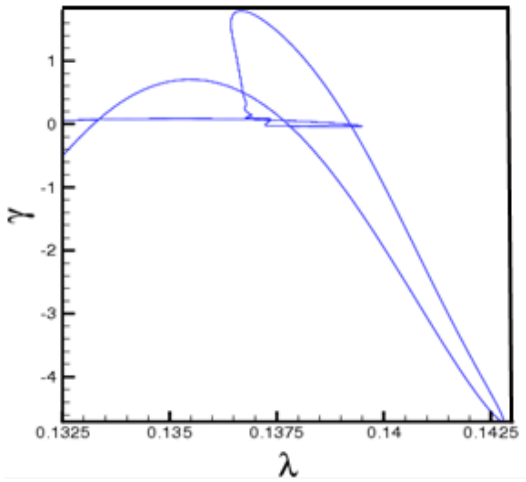

(b)

Figure 8. (a) Multi-periodic flow characteristics, (b) Phase trajectory for $Tr = -200$.

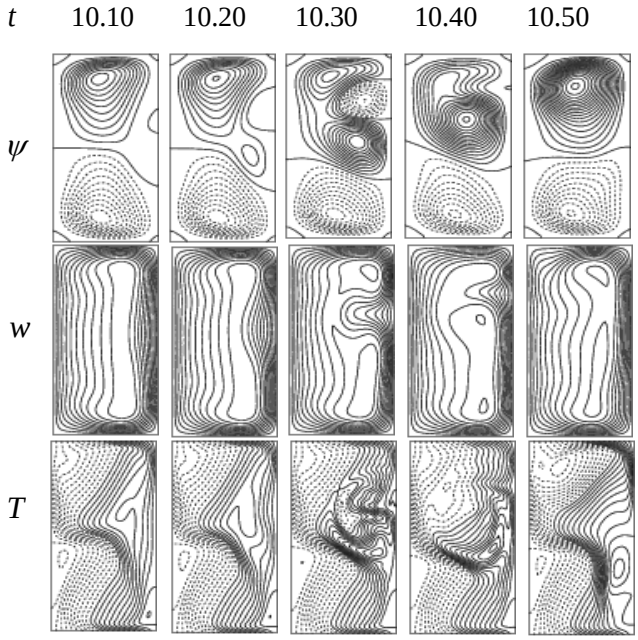

Figure 7. Streamlines of secondary flow *(ψ)*, axial flow *(W)* and isotherm *(T)* for different time (*t*) at $Tr = -100$.

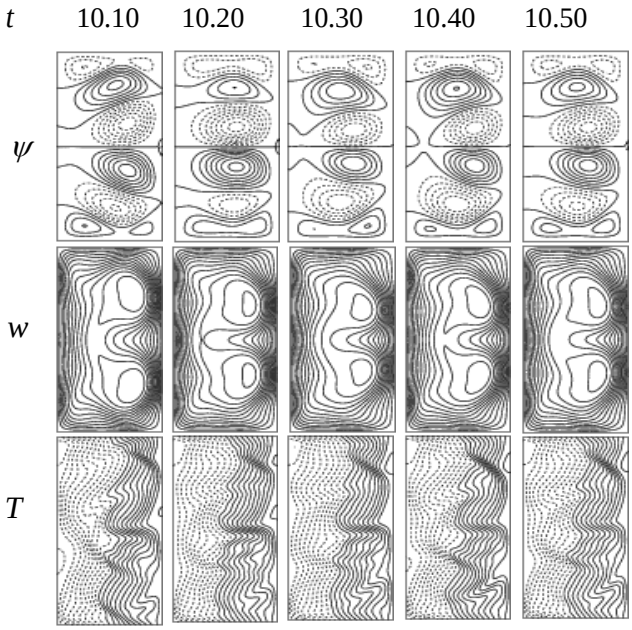

Figure 9. Streamlines of secondary flow *(ψ)*, axial flow *(W)* and isotherm *(T)* for different time (*t*) at $Tr = -200$

To analyze the formation of the secondary flow structure and axial velocity, contours of streamlines, axial velocity and temperature profiles are represent in Figure 3 for $Tr = 0$ at time $5 \le t \le 10.45$, in Figure 5 for $Tr = -50$ at time $10 \le t \le 10.50$, in Figure 7 for $Tr = -100$ at time $10 \le t \le 10.50$, in Figure 9 for $Tr = -200$ at time $10 \le t \le 10.50$, in Figure 11 for $Tr = -335$ at time $16 \le t \le 16.50$, in Figure 13 for $Tr = -340$ at time $15 \le t \le 19.10$ and in Figure 15 for $Tr = -340$ at time $10 \le t \le 10.120$, respectively. The secondary flow form two opposing re-circulating locations: one is outer flow (clockwise), as indicated by the thick lines, and the other is inner flow (clockwise), as indicated by the scattered lines. These line curves are affected owing to the united operation of the centrifugal, Coriolis, and buoyancy forces. Centrifugal force has formed because of flow over the duct, while Coriolis force is caused for rotation of the channel around the *y*-direction. The buoyant force is incorporated for the thermal gradient of the curved duct. In this study, it is obtained that the transition of the secondary velocity at $Tr = 0$ depicts in the three-, four- and six-vortex solutions. At $Tr = -50$ the vortex structure demonstrates in the two-, three-, four- and five-vortex solutions; at $Tr = -100$ it oscillates in the six-, seven-, eight- and multi-vortex solutions, at $Tr = -200$ the flow reveals in the six- and eight-vortex solutions; at $Tr = -335$ it exposes in the two-, three-, five- and multi-vortex; at $Tr = -340$ shows in the three- four- and five-vortex solutions and at $Tr = -400$ the flow oscillates in the three-, four- and five-vortex solutions. It is further found from the isotherms that the overall heat transfer is increased with the increase of rotation. The highly complex secondary flow filed is developed with higher Taylor number, and the heat trasfer is boosted substantially by the chaotic solutions than the other.

In this study, fluid is accelerated under joint action of the centrifugal, Coriolis and buoyancy forces. As seen in the figures of the secondary flow (SF) patterns, the SF consists of asymmetric solutions. With heating and cooling the walls changes of fluid density that induce thermal convection in the fluid; the resulting flow behavior is, therefore, determined by the combined action of the radial flow caused by the centrifugal body force and the convection caused by the buoyancy force due to temperature variation between the horizontal walls.

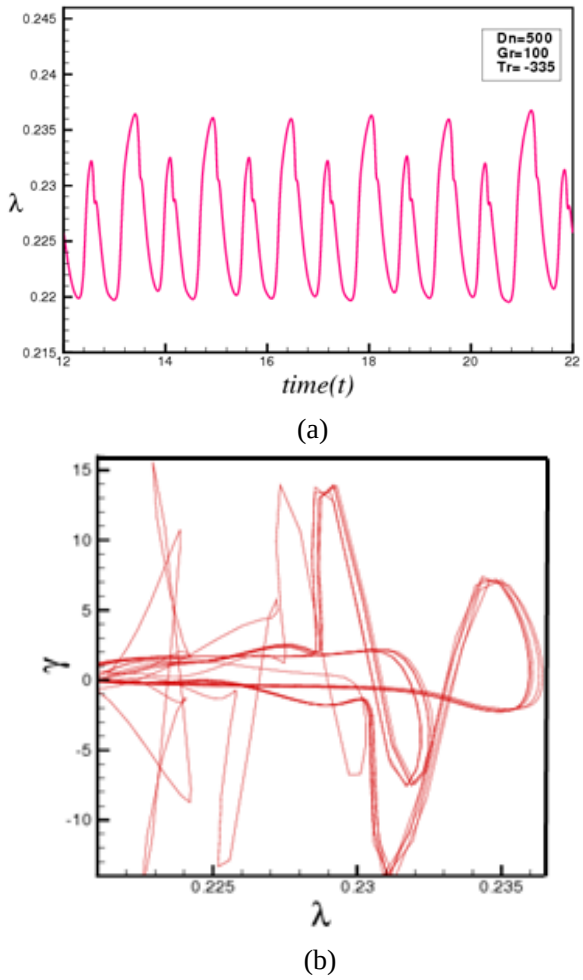

Figure 10. (a) Chaotic flow characteristics (b) Phase trajectory for $Tr = -335$.

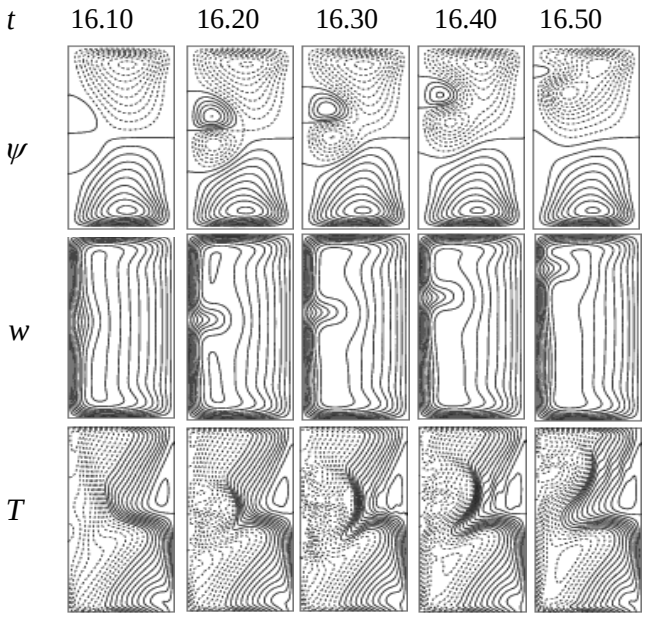

Figure 11. Streamlines of secondary flow (Ψ), axial flow (w) and isotherm (T) for different time (t) at $Tr = -335$.

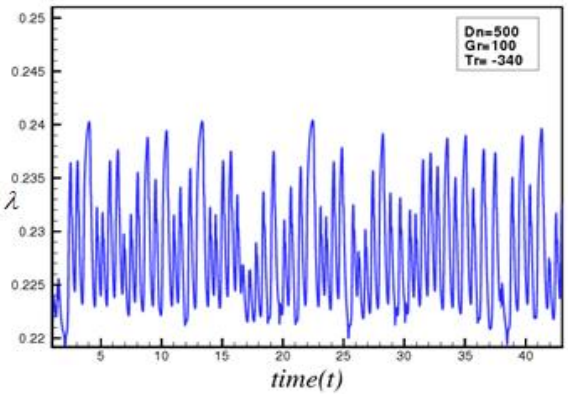

(a)

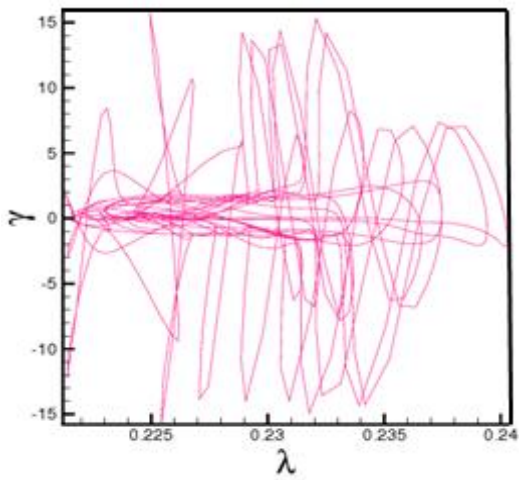

(b)

Figure 12. (a) Chaotic flow characteristics (b) Phase trajectory for $Tr = -340$.

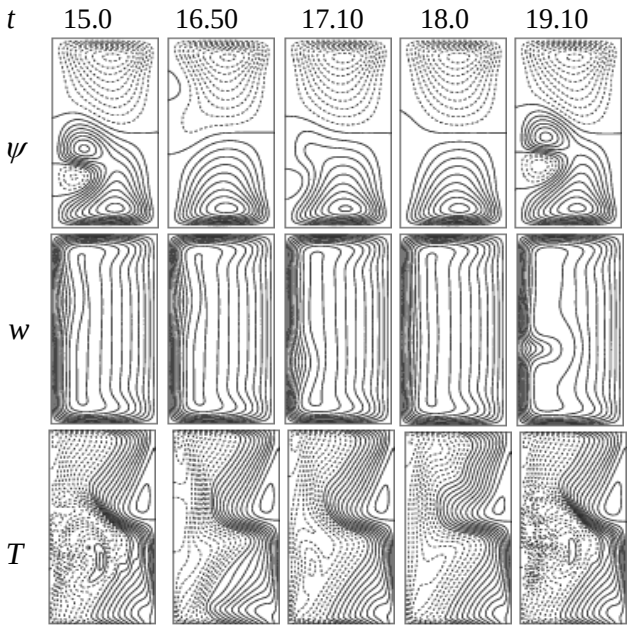

Figure 13. Streamlines of secondary flow *(ψ)*, axial flow *(w)* and isotherm *(T)* for different time (*t*) at $Tr = -340$.'

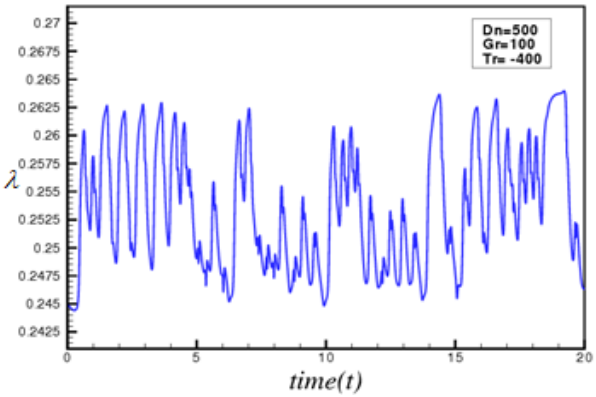

(a)

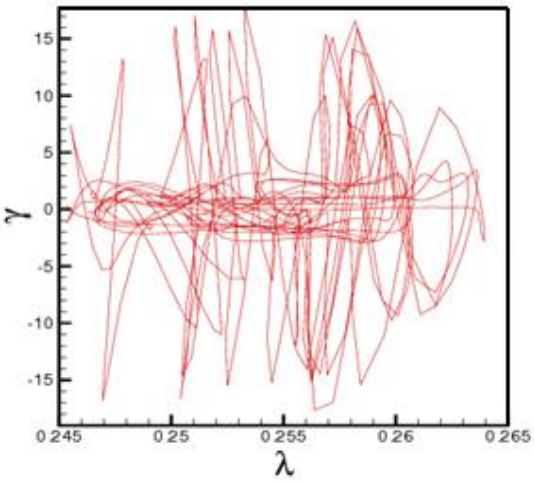

(b)

Figure 14. (a) Chaotic flow characteristics (b) Phase trajectory for $Tr = -400$.

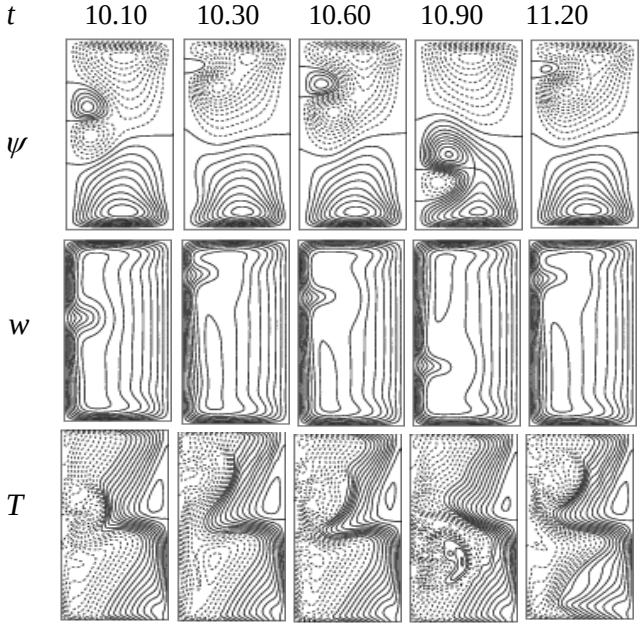

Figure 15. Streamlines of secondary flow *(ψ)*, axial flow *(w)* and isotherm *(T)* for different time (*t*) at $Tr = -400$.

The present study shows that the secondary flow consists of asymmetric solutions. The reason is that heating the outer wall causes deformation of the secondary flow and yields asymmetry of the flow. With the heating and cooling the sidewalls changes of fluid density that induce thermal convection in the fluid; the resulting flow behavior in the cross section is, therefore, determined by the combined action of the radial flow caused by the centrifugal body force and the convection caused by the buoyancy force due to temperature difference between the walls. In this regard, it should be noted that Mondal *et al*. (2016, 2015) conducted numerical simulation of viscous incompressible flow and heat transfer through a rotating curved square-shaped channel with constant curvature and small curvature, and identified transitional behavior of the flow with vortex structure of secondary flows. As seen in the temperature contours, the enhancement of heat transfer for chaotic flow is more effective than the other flow states because of the generation of substantial number of secondary vortices near the concave wall for the chaotic flow. The centrifugal and buoyancy forces influence the overall flow pattern and Dean vortices. In this study, it is observed that the number of secondary vortices increases for chaotic flow and reached at the highest number compared to other cases. As *Tr* is increased in the negative direction, the fluid particles move in the vicinity of the wall and make friction to each other; at a certain time, Dean vortices are constructed yonder the wall of the channel which plays an outstanding responsibility in transferring heat from the outer wall to the fluid.

4.2 Convective heat transfer

To examine convective heat transfer from the hot wall to the fluid, a comprehensive temperature gradient is calculated for both the walls. Figures 16(a) and 16(b) show the corresponding temperature drop with different *Tr* for the cool and hot wall, respectively. The temperature gradient for the cooled wall for different *Tr* reports higher temperature drop at the centre of the wall (y = 0). The centrifugal force and corresponding convective heat generation to the outward direction influence the heat transfer at the centre of the wall. On the contrary, the temperature gradient shows an increasing trend near the wall irrespective to *Tr*. The secondary flow in the inward direction and corresponding convective heat transfer influences the temperature drop near the wall. For the heated wall, the temperature gradient for different *Tr* shows a similar increasing trend and the temperature gradient is found maximum at the centre of the domain.

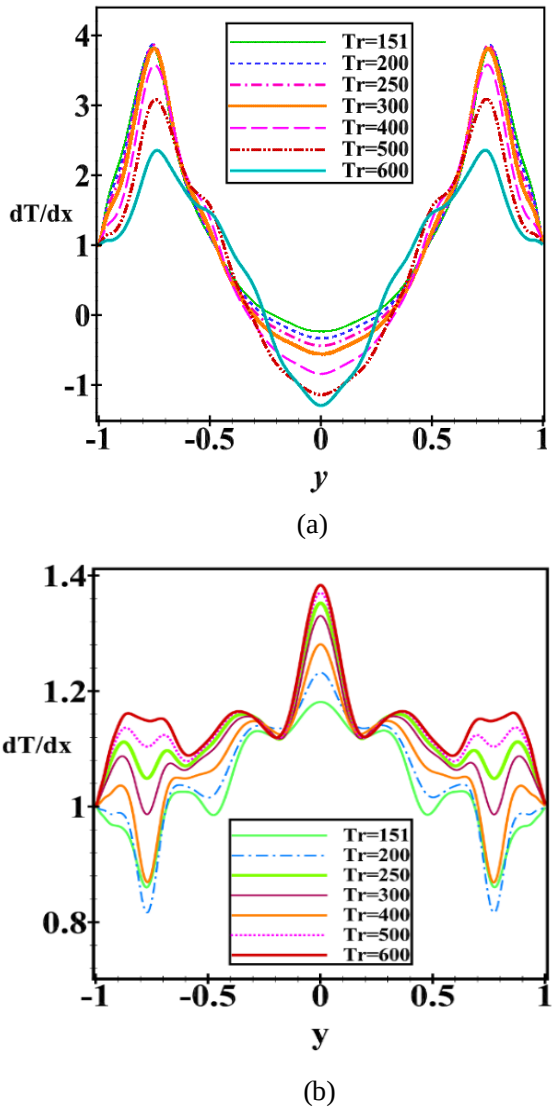

Figure 16. (a) Temperature gradients at the (a) cooled wall and (b) heated wall.

4.3 Validation of the numerical results

Here, a comparative study between the numerical and experimental investigations is provided for both curved square and rectangular duct flow. Figure 17(a) presents a relative comparison of our numerical findings with the laboratory-based experiment by Yamamoto *et al.* (2006) of rotating curved square duct flow for negative rotation at $Tr = -150$, while Figure 17(b) shows a comparative study of our numerical result with the with the laboratory-based experimental investigation obtained by Chandratilleke (2001) for the flow through a stationary curved rectangular duct of aspect ratio 2 at *Gr* = 500. As seen in Figures 17(a) and 17(b), our numerical results have a good agreement with the experimental investigations.

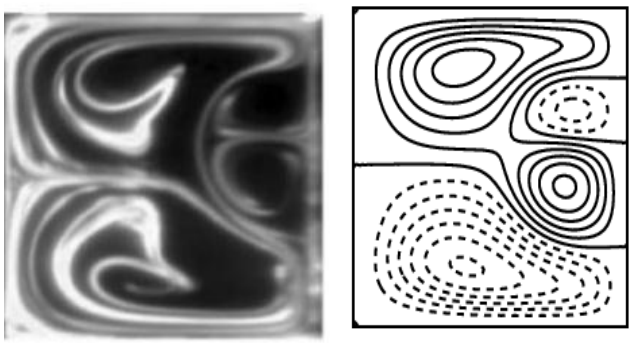

Dn = 321 *Dn* = 520

(a)

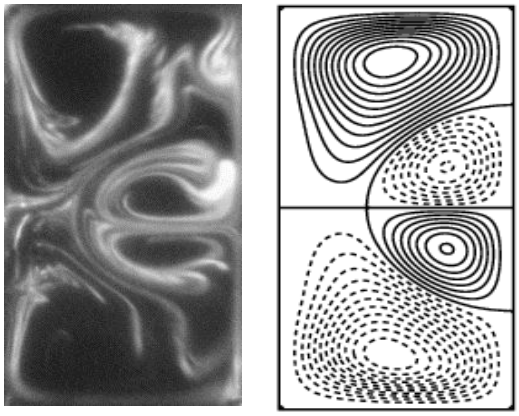

Dn = 262 *Dn* = 265

(b)

Figure 17. Validation of the numerical result (right) with experimental (left), Experimental study by (a) Yamamoto *et al*. (2006), (b) Chandratilleke (2001).

5. Conclusion

The ongoing study determines a spectral-based numerical approach on fluid flow and heat conduction through a curved duct with negative rotation. A wide-range of the Taylor numbers *Tr* ranging from -500 to 0 is considered for curvature ratio 0.2 and aspect ratio 2. The numerical findings are validated with the available experimental data. The following conclusions are drawn from the present study:

- Time-history as well as phase space analysis demonstrates that transient flow develops in the consequence "*chaotic → periodic → multi-periodic → chaotic*", for co-rotating case.
- Velocity contours show that there exist 2-vortex for the steady-state, 2- to 6-vortex for the periodic or multi-periodic oscillation while 2- to 8-vortex for the chaotic oscillation.
- Convective heat transfer is increased with the increase of rotation. The highly complex secondary flow filed is developed with higher *Tr*, and heat transfer is enhanced substantially by the chaotic solutions than other flow state.
- The current study shows that there arises a strong interaction between the heating-induced buoyancy force and the centrifugal-Coriolis instability in the rotating curved channel that stimulates fluid mixing and thus increases heat transfer in the fluid**.**

Acknowledgment: The authors would like to gratefully acknowledge the financial support from Jagannath University through JnU research grant (জবি/গবেষণা/গপ্র/২০২০-২০২১/বিজ্ঞান/২৬) to conduct this research work.

References

Abu-Hamdeh NH, Bantan RAR, Tlili I. (2020). Analysis of the thermal and hydraulic performance of the sector-by-sector helically coiled tube heat exchangers as a new type of heat exchangers. *International Journal of Thermal Sciences*, 150: 106229.

Bibin KS, Jayakumar JS. (2020). Thermal hydraulic characteristics of square ducts having porous material inserts near the duct wall or along the duct centre. *International Journal of Heat and Mass Transfer*, 148: 119079.

Chanda RK, Uddin MK. Mondal RN. (2021a). A Spectral-based Numerical Study on Time-dependent Fluid Flow and Energy Distribution through a Rotating Coiled Rectangular Duct with the Effects of Coriolis Force, *International Journal of Advanced in Applied Mathematics and Mechanics*, 8(3): 48 – 61

Chanda RK. Hasan MS. Lorenzini G. and Mondal RN, (2021b). Effects of Rotation and Curvature Ratio on Fluid Flow and Energy Distribution through a Rotating Curved Rectangular Channel, *Journal of Engineering Thermophysics*, 30(2): 243-269.

Chanda RK, Hasan MS, Alam MM. and Mondal RN. (2021c), Taylor-Heat Flux Effect on Fluid Flow and Heat Transfer in a Curved Rectangular Duct with Rotation, *International Journal of Applied and Computational Mathematics*, 7: 146.

Chandratilleke TT. (2001). Secondary flow characteristics and convective heat transfer in a curved rectangular duct with external heating. 5th World Conference on Experimental Heat Transfer, *Fluid Mechanics*

and Thermodynamics [ExHFT-5], Thessaloniki, Greece.

Chandratilleke TT. and Nursubyakto K. (2003). Numerical prediction of secondary flow and convective heat transfer in externally heated curved rectangular ducts, *Int. J. Thermal Sciences*, 42: 187-198.

Dean WR. (1927). Note on the motion of fluid in a curved pipe. *Philos Mag*., 4: 208-23.

Hasan, MS, Islam MM, Ray SC and Mondal RN. (2019). Bifurcation structure and unsteady solutions through a curved square duct with bottom wall heating and cooling from the ceiling. *AIP Conference Proceedings*, 2121(1): 050003.

Hasan MS, Islam MS, Badsha MF, Mondal RN and Lorenzini G. (2020). Numerical investigation on the transition of fluid flow characteristics through a rotating curved duct. *International Journal of Applied Mechanics and Engineering*, 25(3): 45-63.

Hasan MS, Mondal RN, Kouchi T and Yanase S. (2019). Hydrodynamic instability with convective heat transfer through a curved channel with strong rotational speed. *AIP Conference Proceedings*, 2121 (1): 030006.

Hasan MS, Mondal RN. and Lorenzini, G. (2020). Physics of bifurcation of the flow and heat transfer through a curved duct with natural and forced convection. Chinese Journal of Physics, 67: 428-457.

Hasan MS, Mondal RN. and Lorenzini G. (2019). Numerical Prediction of Non-isothermal Flow with Convective Heat Transfer through a Rotating Curved Square Channel with Bottom Wall Heating and Cooling from the Ceiling. *International Journal of Heat and Technology*, 37(3): 710-720.

Hasan MS, Mondal RN and Lorenzini G. (2019). Centrifugal Instability with Convective Heat Transfer through a Tightly Coiled Square Duct. *Mathematical Modelling of Engineering Problems*, 6(3): 397-408.

Ludwieg H. (1951). Die Ausgebildete kanalstromung in einemrotierenden System. *Ing.-Arch*. 19: 296-308.

Miyazaki H. (1971). Combined free and force convective heat transfer and fluid flow in a rotating curved circular tube. *Int. J. Heat Mass Transfer*, 14: 1295-1309.

Miyazaki H. (1973). Combined free and force convective heat transfer and fluid flow in rotating curved rectangular tubes. *Trans. ASMEC: Heat Transfer*, 95: 64-71.

Mondal RN, Kaga Y, Hyakutake T, Yanase S. (2006). Effects of curvature and convective heat transfer in curved square duct flows. *Trans. ASME, Journal of Fluids Engineering*, 128(9): 1013-1022.

Mondal RN, Kaga Y, Hyakutake T and Yanase S. (2007a). Bifurcation Diagram for Two-Dimensional Steady Flow and Unsteady Solutions in a Curved Square Duct. *Fluid Dynamics Research*, 39: 413-446.

Mondal RN, Alam MM and Yanase S. (2007b). Numerical Prediction of Non-Isothermal Flows through a Rotating Curved Duct with Square Cross Section. *Thammasat Int. J. of Science and Technology*, 12: 24-43.

Mondal RN, Uddin MS and Yanase S. (2010). Numerical Prediction of Non-Isothermal Flow through a Curved Square Duct. *Int. J. Fluid Mech. Research*, 37: 85-99.

Mondal, RN, Islam MS, Uddin MK and Hossain MA. (2013). Effects of Aspect Ratio on Unsteady Solutions through a Curved Duct Flow, *Int. J. Appl. Math. & Mech.*, 34(9), 1-16.

Mondal, RN. Ray SC. and Yanase S. (2014). Combined Effects of Centrifugal and Coriolis Instability of the Flow through a Rotating Curved Duct with Rectangular Cross Section. *Open Journal of Fluid Dynamics*, 4: 1-14.

Mondal RN, Ray SC. and Yanase S. (2015a). Combined effects of centrifugal and Coriolis instability of the flow through a rotating curved duct with rectangular cross section. *Open J. Fluid Dynamics*, 4(4): 1-14.

Mondal RN, Islam MZ, Islam MM and Yanase S. (2015b). Numerical Study of Unsteady Heat and Fluid Flow through a Curved Rectangular Duct of Small Aspect Ratio. *Thammasat Int. J. Sci. and Tech.*, 20(4): 1 - 20.

Mondal, RN, Helal, MNA and Ghosh, BP. (2016). Numerical Simulation of Viscous Incompressible Fluid Flow and Heat Transfer through a Rotating Curved Square Channel, *American Journal of Fluid Dynamics*, 6(1): 1-10.

Mondal RN, Watanabe T, Hossain MA, Yanase S. (2017). Vortex-Structure and Unsteady Solutions with Convective Heat Transfer trough a Curved Duct. *Journal of Thermophysics and Heat Transfer*, 31(1**):** 243-254.

Mondal, RN, Hasan MS, Islam, MS, Islam MZ, Saha SC. (2021). A Computational Study on Fluid Flow and Heat Transfer through a Rotating Curved Duct with Rectangular Cross Section, *Int. J. of Heat and Technology*, 39(4): 1213-1224.

Adhikari SC, Chanda RK, Bhowmick S, Mondal RN, Saha SC. (2021). Pressure-induced instability characteristics of a transient flow and energy distribution through a loosely bend square duct, *Energy Engineering*, 119(1): 429-451.

Nobari MRH, Ahrabi BR, Akbari G. (2009). A numerical analysis of developing flow and heat transfer in a curved annular pipe. *International Journal of Thermal Sciences*, 48: 1542–1551.

Nowruzi H, Ghassemi H and Nourazar SS. (2019). Linear Hydrodynamic Stability of Fluid Flow in Curved Rectangular Ducts: Semi-Analytical Study. *Journal of Mechanics*, 35(5): 747-765.

Wang LQ and Chang KC. (1996). Flow transition and combined free and forced convective heat transfer in rotating curved channels: the case of positive rotation. *Physics of Fluids*, 8: 1-13.

Wang LQ and Yang TL. (2004). Multiplicity and Stability of Convection in Curved Ducts: Review and Progress. *Advances in Heat Transfer*, 38: 203-256.

Wang L and Yang T. 2005. Periodic Oscillation in Curved Duct Flows. *Physica D*, 200: 296-302.

Yanase S., Mondal RN and Kaga Y, (2005), Numerical study of non-isothermal flow with convective heat transfer in a curved rectangular duct, *Int. J. Thermal Sciences*, 44, 1047-1060.

Yanase S and Nishiyama K. (1988). On the Bifurcation of Laminar Flows through a Curved Rectangular Tube. *Journal of Physical Society of Japan*, 57: 3790-3795.

Yanase S, Watanabe T, Hyakutake T. (2008). Traveling-wave solutions of the flow in a curved-square duct. *Physics of fluids*, 20: 124101.

Yamamoto K, Xiaoyun W, Kazuo N and Yasutaka H. (2006). Visualization of Taylor-Dean flow in a curved duct of square cross section. *Fluid Dynamics Research*, 38: 1-18.

Zhang C, Niu Y and Xu J. (2020). An anisotropic turbulence model for predicting heat transfer in a rotating channel. *International Journal of Thermal Sciences*, 148: 106119.

Zhang J, Zhang B and Ju J. (2001). Fluid flow in a rotating curved rectangular duct. *Int. J. Heat Fluid Flow*, 22(6): 583-592.

Zhao H, Li X, Wu Y and Wu X. (2020). Friction factor and Nusselt number correlations for forced convection in helical tubes. *International Journal of Heat and Mass Transfer*, 155: 119759.